

An effect of Manganese and Nickel in VVER-440 reactor pressure vessel steels during the process of annealing

Jana Simeg Veternikova^{1, a)}, Matus Hupka¹⁾, Stanislav Sojak¹⁾, Martin Petriska¹⁾
and Vladimir Slugen¹⁾

Author Affiliations

¹ Slovak University of Technology, Faculty of Electrical Engineering and Information Technology, Institute of Nuclear and Physical Engineering, Ilkovicova 3, 841 04 Bratislava.

Author Emails

^{a)} Corresponding author: jana.veternikova@stuba.sk

Abstract. In this paper, an effect of thermal stress on VVER-440 reactor pressure vessel steel (15KhMFAA) was observed by non-destructive Positron Annihilation Lifetime Spectroscopy and Coincidence Doppler Broadening Spectroscopy. This steel was investigated previously in a couple of publications, but the influence of the thermal treatment was studied mostly up to 500 °C. Our recent positron results from the optimization of the recovery annealing temperature published in [1] indicated that the structure is significantly changed at temperatures over 500°C, although the reason was not in charge of structural defects on which positrons are sensitive. This paper studies closer the chemical aspects of the annealing and the formation of precipitates at temperature of 550°C. The results indicated an effect of manganese and nickel on the structure surrounding structural defects which is changing during the process of the annealing.

INTRODUCTION

The reactor pressure vessel (RPV) of the nuclear power plant (NPP) is not replaceable, thus it limits the lifetime of the NPP and the possibility to extend its operating time. The RPV of VVER-440 manufactured from steel 15KhMFAA (chemical composition in Table 1) is exposed by radiation flux up to 10^{-24} m⁻² and temperature under 300 °C during the whole projected lifetime. The material of RPV is changed due to the radiation-induced defects and precipitates as well as thermally-induced precipitates. The long-term thermal stress contributes slighter to the microstructural changes than the effect of the irradiation, but their combination is evident, and both are the most intensive in the first period of the exposition [2].

TABLE 1. Chemical composition of VVER-440 reactor pressure vessel steel – 15KhMFAA in % wt.

| Cr | Mn | Mo | Ni | Si | C | V | S and P | Cu |
|-------|---------|---------|---------|-----------|-----------|-----------|-----------|----------|
| 2-2,5 | 0,3-0,6 | 0,6-0,8 | max 0,4 | 0,17-0,37 | 0,11-0,16 | 0,25-0,35 | max 0,015 | max 0,08 |

The microstructural changes of RPV due to irradiation can be partially annealed out, mostly needed as a recovery of welds, and thus the RPV's lifetime can be extended. The RPV of VVER-440 are ordinary recovery annealed at 475 °C during \approx 150 hours for recombination of radiation-induced defects. However, this recovery is only partial while precipitations located on grain boundaries are stable at this temperature. The Cu and P precipitates obviously enriched by Si, Ni and Mn are merging to the bigger ones with lower density at temperature between 300 and 500 °C [3, 4], thus this worsens the mechanical properties mostly during the irradiation. Precipitates of P and Cu enriched by Ni and Nb start to dissolve over 500 °C and enriched by Mo, Cr and Mn over 600°C [5, 6].

The RPV of VVER-1000 will be annealed at higher temperatures of 565°C due to its thicker wall than in VVER-440. The next reason is a complex recovery at this temperature, as there is defect recombination together with the partial dissolution of precipitates there. The RPV of VVER-1000 with higher nickel content, operating at a higher temperature (290°C) than VVER-440 (260°C), has a problem with Ni and Mn precipitates [2], which are commonly located near the radiation-induced defects in complex Mn-Ni-Si [7]. However, over the temperature of 510 °C, the

precipitation of carbides (mostly Cr_{23}C_6) starts. They are stable and can segregate on grain boundaries up to the temperature of dissolution $\approx 780\text{ }^\circ\text{C}$ [8, 9]. Thus, the structure can be more coarsened here due to annealing, which consequently worsens the mechanical properties.

Nickel with the content above 1% wt. can increase the susceptibility to temper embrittlement similar as Cu and P [10]. This is less distinctive for steel with lower nickel content and the comparable presence of Cu and P. Thus, the RPV material of VVER-440 should be more stable and its temper embrittlement should be negligible as Cu and P contents are strictly limited for the newer RPVs (V213). However, the older RPVs of VVER-440 (V230) with no limited content of P and Cu had to be recovery annealed within the period of the projected lifetime (up to 40 years). In the future, the recovery process will be probably common for all RPVs as the lifetime is extended to 60+ years.

In this paper, reactor pressure vessel steel of VVER-440 was annealed at $550\text{ }^\circ\text{C}$ for 2 hours in terms of thermal stress observation by very sensitive non-destructive techniques – Positron annihilation lifetime spectroscopy (PALS) and Coincidence Doppler Broadening spectroscopy (CDBS), which can find very small change in the microstructure. The PALS technique can determine the type of defects in the structure and CDBS techniques are sensitive to the chemical surrounding of the defects.

EXPERIMENTAL METHODS AND TREATMENTS

The PALS technique is a very sensitive non-destructive technique available to detect small vacancy defects (mono- and di-vacancies) with a concentration of 1 ppm and more. The PALS measurement was performed at digital apparatus with a digital DRS4 card for recording and evaluating the data [11]. The experimental positron lifetime, the time difference between the positron's birth and its annihilation, is obtained and compared to the calculated theoretical values. The positron data were treated according to the Standard Trapping Model [12], where three positron lifetimes are separated from the measured spectrum. The first lifetime match to the material bulk value. The second positron lifetime describes the structural defects and increases with the defect size growth. The third component, lifetime 3, answers to the background of the annihilation (annihilation out of the sample). The data were treated in the LT9 program designed by J. Kansy [13].

The Coincidence Doppler Broadening Spectroscopy (CDBS) is also a positron technique where only the annihilation energy spectrum is observed and further evaluated. The annihilation spectrum with the shape of a Gaussian can be changed due to the presence of defects. The peak of the spectra (S parameter) is increasing with a growth of defect size or defect concentration. The spectrum is also affected by the chemical surroundings of the annihilation place, which is determined by the wings area of the spectrum (W parameter). The W parameter can be compared to reference spectra of variable chemical elements, and the presence of the chemical element near the vacancy defect can be thus confirmed. The annihilation spectrum depends on the chemical composition of the material since positrons are attracted not only to defects but also to some chemical elements. The attractivity of positron annihilation in a chemical element describes the positron affinity (eV). The positron affinity (see Table 2) is a value of energy that needs to be released or received during the process of atom–positron interaction. The CDBS was measured by the semi-conductor detectors with a liquid nitrogen cooling system [14]. The data was treated in CDBTool software designed by M. Petriska [15].

TABLE 2. Values of the positron affinity for chemical elements in 15KhMFAA [16, 17].

| Chemical element | Affinity [eV] | Positron lifetime [ps] | Content [wt%] |
|------------------|---------------|------------------------|---------------|
| Fe | -2,68 | 110 | Bal. |
| Cr | -2,27 | 105 | 2,5 |
| Mn | -2,57 | 109 | 0,5 |
| Ni | -2,91 | 108 | 0,4 |
| Mo | -1,88 | 106 | 0,5 |

The sample of 15KhMFAA was firstly measured in the as-received state, and then thermal stress was applied at temperatures of $550\text{ }^\circ\text{C}$ for 2 hours. The sample was then observed by PALS and CDB techniques for determination of structural stress and deformation in the form of expected vacancy-type defects. The changes were small, but they were visible for these techniques.

RESULTS

The positron lifetime was measured for the as-received sample and then for the sample after the annealing at 550°C for 2 hours. The results are shown in Table 3. The first component, the bulk value, was fixed at 110 ps (the value for pure Fe). The second component of the fitted spectra was between 150 and 160 ps for both samples, which responds mostly to dislocations. The intensity of the second lifetime (I2), which is proportional to defect concentration, was smaller for the annealed sample, about $8,1 \pm 4,9$ %. This could indicate an effect of the recovery in the structure due to annealing during which defects could have been partially recombined. However, the average lifetimes have almost the same value in the range of error bars, which describes that no distinctive change was probably made. The change in I2 could be also explained by a change in microstructure due to the annealing and due to formation of precipitations, probably from Mn, Cr or Ni, which positron affinity is comparable to Fe.

TABLE 3. Positron lifetimes for the investigated samples.

| Sample | Lifetime of defects | Intensity for LT2 | Average lifetime [ps] |
|-------------|---------------------|-------------------|-----------------------|
| | LT2 [ps] | I2 [%] | |
| As-received | 154 ± 1 | $75,8 \pm 3,2$ | 141 ± 2 |
| Annealed | 160 ± 2 | $67,7 \pm 1,8$ | 139 ± 2 |

The chemical surroundings of the positron annihilation site were observed by the CDBS technique. Although the PALS results did not show a significant change in the structure of the samples, the CDBS shows differences in the S and the W parameters (see Figure 1). For better visualization, the S and the W values are normalized according to the pure Fe. Three samples of the as-received material were observed, and the data were similar with the dispersion of 2%. The annealed sample was shifted to a higher S parameter and a lower W parameter, but in the line between the pure iron and the pure manganese. The values for the reference Cr, Mo, and Ni were sufficiently diverted to the Fe–samples line, thus we can assume that mostly Mn has a sufficient effect on positrons here.

In the Figure 1, the as-received samples are not on the Fe–Mn line and are slightly shifted to the value of the single vacancy, which can indicate the presence of small defects such as dislocation. The annealed sample is on the Fe–Mn line, which could explain the significant effect of Mn or the presence of Mn near the position annihilation site (near existed dislocations).

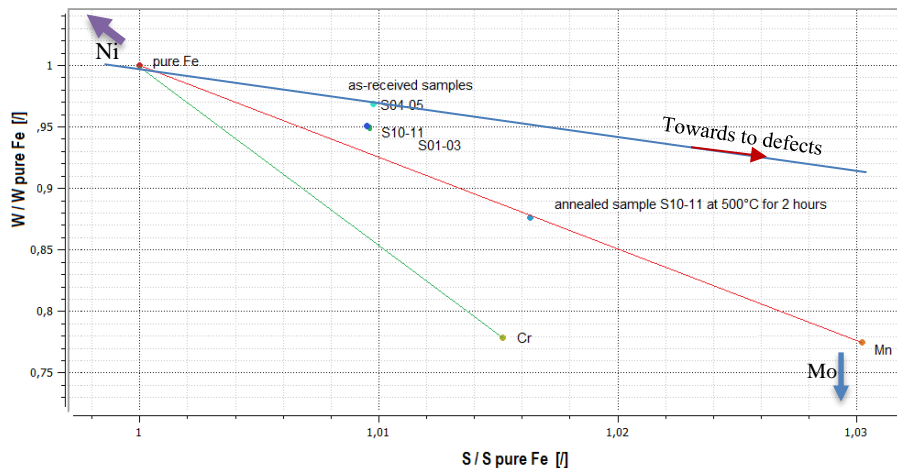


FIGURE 1. Normalized W-S diagram to pure Fe for the as-received and annealed sample and reference elements Mo, Mn, Ni and Cr.

The Mn effect is also shown in Figure 2 (a, b, c, d, e), where is displayed a comparison of the annihilation spectra for the as-received sample and the individual reference elements (Mn, Mo, Ni, Cr). From this, the most similar behavior of the analyzed spectra with manganese is evident here.

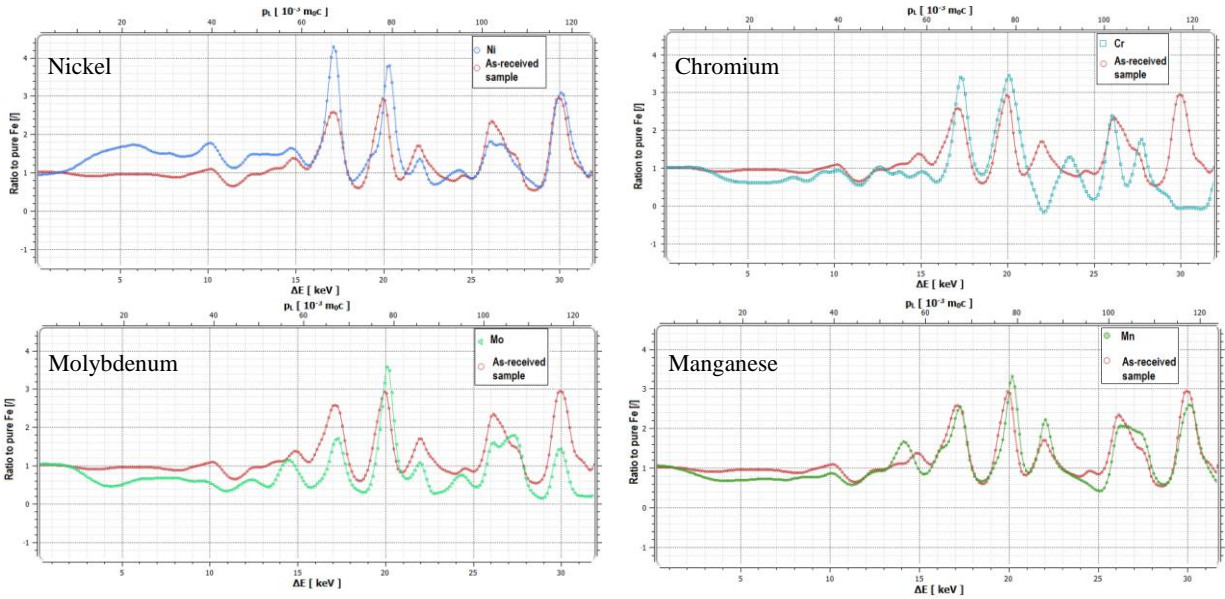


FIGURE 2. Comparison of the normalized CDB spectra for as-received sample with the pure chemical elements – Mo, Ni, Cr and Mn. The error bars are not considered for simplification.

Detailed behaviors of the CDB spectra in the margins of the S and the W parameters are presented in Figure 3. The S parameter, including the energy with the shift of up to 2 keV from the annihilation energy 511 keV, shows that the as-received sample as well as the annealed sample do not contain significant concentrations of vacancies. The curves calculated for single vacancy and vacancy cluster (9 vacancies) from [18] are distinctive over their S values. The shift to the higher S parameter can be due to the presence of dislocations or, eventually, the influence of the manganese surrounding the dislocations.

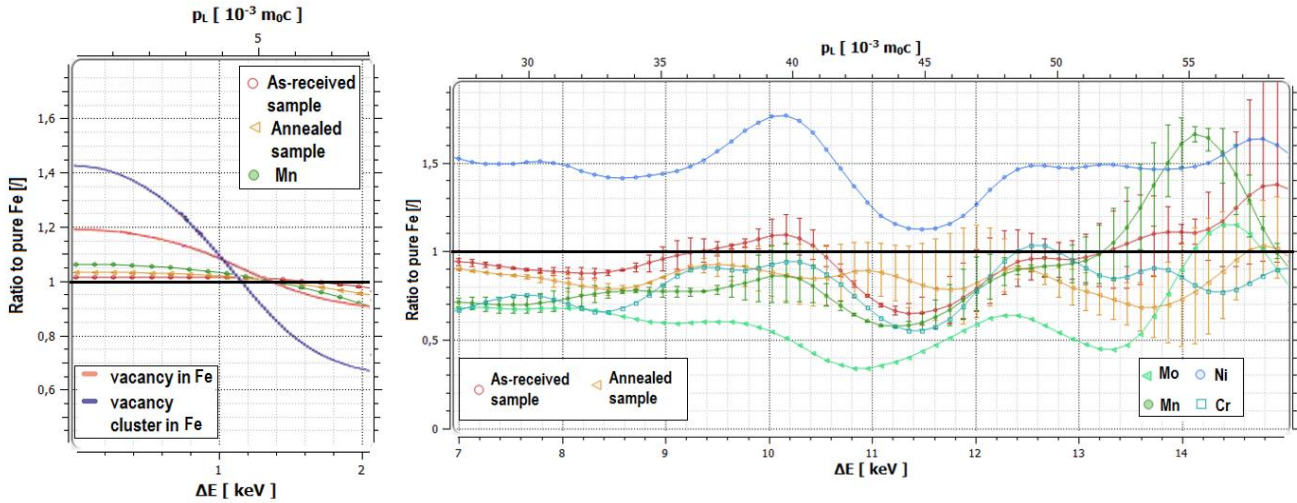


FIGURE 3. CDBS spectrum shown in the merges of the S parameter and the W parameter for the as-received and the annealed samples and for the reference samples: pure elements Mo, Ni, Mn, and Cr.

The W parameter for the as-received and the annealed sample, describing the energy shift between 7 and 15 keV from the annihilation energy of 511 keV, has similar behavior as the reference Mn for a first look. Although, Ni plays probably also a role in the behavior of the investigated samples, which is more evident from the shape of the curve at energies over 13 keV and according to the higher values (over 1) around the energy of 10 keV. The annealed sample is still under the value of 1 and is probably less affected by nickel than the as-received sample. This could be due to

the partial dissolution of precipitates with nickel in the structure over 550 °C and its more homogenous distribution (not only near the dislocations). The effect of Mn probably still stays here but is slightly suppressed in energies over 12 keV, where Fe or Cr effect starts to be visible more.

CONCLUSION

In this paper, the thermal stress was applied to the reactor pressure vessel steel of VVER-440 (15KhMAA). The annealing at the temperature limited for starting of the dissolution of S, P and Ni precipitates was applied. It is a similar temperature for VVER-1000 recovery annealing for complex structural regeneration (defect recombination as well as precipitates dissolution). The PALS results indicated that the dislocations were probably stable or were annealed out only in a very low almost negligible amount (in terms of the error bars) during the annealing. This was expected as minimum defects were in the sample as no previous loading was applied there. However, the change in CDBS spectra between the as-received and annealed sample was found in chemistry around the dislocations. In the as-received samples, Ni and Mn seem to play an important role and after the annealing, their effect was probably suppressed. The annealed sample showed closer behavior to Mn or Cr, respectively. This is in good agreement with the theory when the dissolution of Manganese needs temperatures over 600 °C, and Cr precipitates (carbides, nitrides) are common from 510 to 780 °C. Thus, the influence of nickel and manganese is similar to the effect in VVER-1000, but in a smaller range which is detectable only by very sensitive techniques.

ACKNOWLEDGMENTS

This research was funded by the European Commission—Project DELISA-LTO (No.101061201).

REFERENCES

References should be numbered using Arabic numerals followed by a period (.) as shown below and should follow the format in the below examples.

1. V. Slugen, T. Brodziansky, J. S. Veternikova, S. Sojak, M. Petriska, R. Hinca, G. Farkas, *Materials* **15**, 7091 (2022).
2. B. Gurovich, E. Kuleshova, Y. Shtrombakh, S. Fedotova, O. Zabusov, K. Prikhodko, D. Zhurko, *J. Nucl. Mat.* **434**, 72-84 (2013).
3. O.O. Zabusov, E.A. Krasikov, M.A. Kozodaev, A.L. Suvorov, P. Pareige, B. Radiguet, *VANT, Ser.: Phys. Radiat. Damage Radiat. Mater. Sci.* **3**, 66-72 (2003).
4. P. Pareige, B. Radiguet, A. Suvorov, M. Kozodaev, E. Krasikov, O. Zabusov, *Surf. Int. Anal.* **36**, 581-584 (2004).
5. B.A. Gurovich, E.A. Kuleshova, Yu.A. Nikolaev, *J. Nucl. Mater.* **246**, 91-120 (1997).
6. C. Rowolt, B. Milkereit, A. Springer, C. Kreyenschulte, O. Kessler, *J. Mater. Sci.* **55**, 13244–13257 (2020).
7. K. Murakami, *J. Nucl. Mat.* **542**, 152508 (2020).
8. Z. Li, P. Jia, Y. Liu, H. Qi, *Metals* **9**, 916 (2009).
9. J. M. Vitek, R. Klueh, *Metal. Mat. Trans. A* **16**, 1047-1055 (1983).
10. J. Brynda, V. Cerny, R. Konop, “VVER reactor pressure vessel materials database and monitoring of ageing and lifetime evaluation”, in IAEA publication, Paper – Ageing 2002 Varna. [Online, cit. 25.3.2023], <https://inis.iaea.org/collection/NCLCollectionStore/_Public/33/070/33070705.pdf>.
11. M Petriska, S Sojak and V Slugen, *J. Phys.: Conf. Ser.* **505**, 012044 (2014).
12. R. Krause-Rehberge, S.H. Leipner, *Positron annihilation in Semiconductors* (Springer, Berlin Germany, 1998).
13. J. Kansy, *Nucl. Instr. Meth. Phys. Res. A* **374**, 235 (1996).
14. M. Petriska, V. Sabelova, V. Slugen, S. Sojak, M. Stacho, J. Veternikova, *Phys. Proc.* **35**, 117-121 (2012).
15. M. Petriska, V. Sabelova, V. Slugen, *Defect and Diffusion Forum (Trans. Tech. Publication)* **373**, 71-74 (2017).
16. M. J. Puska, P. Lanki, R. M. Nieminen, *J. of Phys.: Condens. Matter* **1**, 6081 (1989).
17. J. M. Campillo Robles, E. Ogando, F. Plazaola, *J. Phys.: Condens. Matter* **19**, 176222 (2007).
18. V. Sabelova, V. Krsjak, J. Kuriplach, Y. Dai, V. Slugen, *J. Nucl. Mat.* **458**, 350-354 (2015).